American Journal of Engineering Research (AJER)
e-ISSN: 2320-0847 p-ISSN : 2320-0936
Volume-12, Issue-6, pp-35-42
www.ajer.org
Research Paper Open Access

Wind generator: Importance, limit and performance of the aerodynamic profile at the sensors entrance

Ulrich Canissius[1]*, Omary Gastro[2], Delphin Tomboravo[1], Ephrem Razafindrakotomanga[3], Tsialefitry Aly Saandy[3]

[1] Laboratoire de Mécanique et de Métrologie - LMM, Ecole Normale Supérieure pour l'Enseignement Technique, ENSET, Université d'Antsiranana, B.P.O, Madagascar
**Corresponding Author: ulrich_canissius@yahoo.fr*
[2] Computer Science department. Apply to Artificial Intelligence systems, Hainan Vocational University of Science and Technology, Haikou, Hainan 571126, China
[3] Laboratoire de Machines Electriques, Ecole Supérieure Polytechnique, Université d'Antsiranana, B.P.O, Madagascar

ABSTRACT: *Authors solve numerically through an implicit finite difference scheme the transfer equations, permanent, laminar and three-dimensional between an isothermal body of revolution, inclined or not, and a Newtonian fluid considered in ascending flow generated by the natural, forced, rotatory and coupled two-by-two convections in order to bring an answer element to the research question which seems less common in the scientific literature at our disposal. Many authors deal with the aerodynamic problems of wind turbines, but these works are often based on the behavior of the blades ignoring the contribution of the often conical and elliptical profile at the wind sensor entrance. In this framework, the theoretical absence allows us to bring in this paper not only the reason for its existence, but also its corresponding limit to the governing thermodynamic quantities allowing to optimize their modules to the good of the turbine stability.*

KEYWORDS: *three-dimensional convection, aerodynamic profile, ellipse and cone of revolution, shape limit, dynamic momentum.*

Date of Submission: 20-05-2023 Date of acceptance: 03-06-2023

NOMENCLATURE

Roman letter symbols

a	thermal diffusivity of the fluid, ($m^2.s^{-1}$)
a'	length of the semi-axis, according to the length: case of ellipsoid, (m)
b	length of the semi-axis, perpendicular to the axis of revolution, (m)
b'	length of the half-axis of the truncated base of the ellipsoid, perpendicular to the axis of revolution, (m)
B	rotation parameter
Cf_u	meridian friction coefficient
Cf_w	azimuthal friction coefficient
Cp	specifique heat capacity at constant pressure of the fluid, ($J.kg^{-1}.K^{-1}$)
Gr	dimensionless Grashof number
L	length of the reference body (cone, ellipsoid), (m)
Nu	local Nusselt number
Pr	Prandtl number
r	normal distance between the M projection from a point P to the axis of revolution, (m)
Re_∞	Reynolds number relative to the speed at infinity U_∞, far from the wall
Re_ω	rotational Reynolds number relative to rotational speed
S_x,S_φ	geometric configuration factors
T_∞	fluid temperature away from the wall, (K)

T_p wall temperature, (K)
V_x velocity component in x direction, ($m.s^{-1}$)
V_y velocity component in y direction, ($m.s^{-1}$)
V_φ velocity component in φ direction, ($m.s^{-1}$)
x, y meridian and normal coordinates, (m)

Greek letter symbols
α body inclination angle, (°)
α_e eccentric angle in the literature, (rad): case of an ellipsoid, (rad)
φ azimuthal coordinate, (°)
ν kinematic viscosity, ($m^2.s^{-1}$)
λ thermal conductivity, ($W.m^{-1}.K^{-1}$)
β volumetric coefficient and thermal expansion, (K^{-1})
μ dynamic viscosity($kg.m^{-1}.s^{-1}$)
θ_o half angle of the cone: case of a cone, (°)
Ω Richardson number
Indice/Exponent
\+ dimensionless variables

I. INTRODUCTION

The fluid flow around the blades of a wind turbine is very complex. A mathematical model is therefore proposed to better present it. In such a situation, the Navier-Stokes equations will be used for this purpose by posing simplifying assumptions facilitating the resolution of the system of equations of continuity, momentum and heat. In this paper, we will focus more on the particle channeling on the possible sensor of the wind motor. Many researchers invest on the physical and aerodynamic behavior of the wind sensor, but so far, we rarely find the works articulating on the necessity of the conical or elliptical shape of common use of the nose of these wind turbines (figure 1). The absence of the above-mentioned profile in an aeromechanical system certainly leads to a depression at the central level of the sensor causing the instability of the turbine. This disturbance can influence not only the design aspect of the mast or its whole system, but also the structure economic dimension.

Figure 1. Conical, elliptical profile at the inlet of the wind sensor, [1].

Among the works listed, there are still many performances on fluid flows around a conical or elliptical profile, but often treated more in the fundamental approach ignoring the practical framework of the research. The scientific concept of these works remains only in the observation leading to correlation or law at the discretion of researchers and usually to meet the subjective and hypothetical perception of each. With respect to this, we bring our contribution through a theory limiting the shape parameters of the questioned profiles responding to the performance of the modern wind turbine.

II. THEORETICAL FRAMEWORK

Since 1953, the general relation on the solutions of an axisymmetric system of an isothermal body was developed by Merk and Prins [2]. They studied the natural laminar thermal convection of the boundary layer type in the vicinity of a smooth cone and observed the body surface condition contributes to the transfer performance and the roughness attenuates the exchange. The effects of transpiration velocity on a laminar boundary layer flow by free convection from a non-isothermal vertical cone were investigated by [3] and they concluded that due to the increase in temperature gradient, the velocity as well as the surface temperature decreases. [4] and [5] investigated the global heat transfer in unsteady laminar natural convection from an isothermal vertical cone using the integral method. Many authors have treated so far, the thermodynamic problems around a cone and ellipsoid immersed in a two-dimensional or three-dimensional, linear or rotational flow [6], [7], [8], [9], [10], [11], [12], [13], [14] and [15], but without alliances with applied research. The same applies to the coupling of convections with various parameters depending on the objective of the authors [16], [17], [18], [19], which make little contribution to the practical side of research. With regard to all these works, the absence of the practical side leads us to a reflection whose objective is to offer a new scientific knowledge on the meaning of the events and the necessity of use of the questioned profile as aerodynamic regulator, often recommended at the entrance of the modern turbine in spite of the absence of the writings of it.

III. THEORETICAL FOUNDATIONS

The physical model consists of a body of revolution (cone and ellipsoid) of length L and inclined at an angle α or not to the vertical. The wall of the body is kept at a constant temperature Tp, different from the temperature T∞ of the fluid away from the wall which is also constant. Figure 2 represents the spatial configuration of the physical model of the system under study.

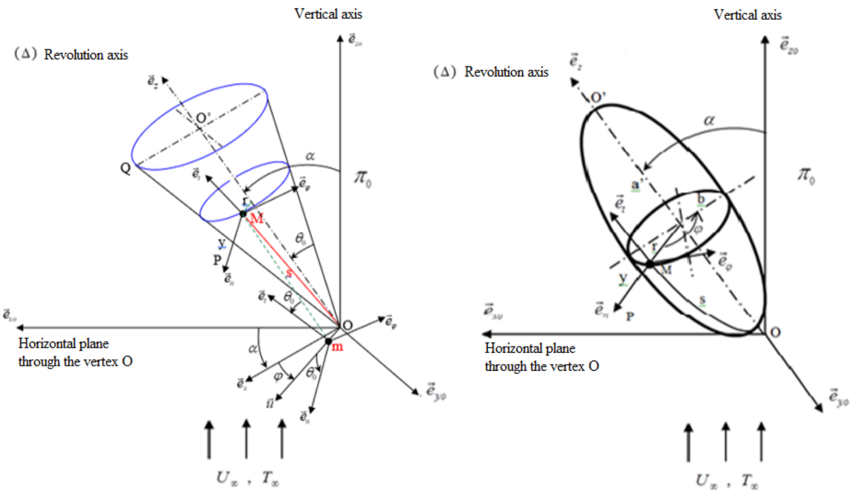

Figure 2. Physical model and co-ordinates system.

IV. CONSERVATION EQUATIONS IN THE BOUNDARY LAYER

The conservation equations are presented in the same way for the two bodies. We only present the case of natural convection and complete with the reference quantities and boundary conditions of the other cases considered (forced, rotary, and the couplings of two by two of the three convections).

a. Case of pure natural convection

Authors pose $\Delta T = T_p - T_\infty$, and the appropriate reduced variables are [20]:

$x_+ = \frac{x}{L}$, $y_+ = \frac{y}{L}Gr^{\frac{1}{4}}$, $\varphi_+ = \varphi$, $V_x^+ = \frac{V_x}{\sqrt{Lg\beta\Delta T}}$, $V_y^+ = \frac{V_y Gr^{\frac{1}{4}}}{\sqrt{Lg\beta\Delta T}}$, $V_\varphi^+ = \frac{V_\varphi}{\sqrt{Lg\beta\Delta T}}$, $r^+ = \frac{r}{L}$ and

$$T^+ = \frac{T - T_\infty}{T_P - T_\infty} \qquad (1)$$

Continuity, momentum and heat equations

$$\frac{\partial V_x^+}{\partial x_+} + \frac{\partial V_y^+}{\partial y_+} + \frac{1}{r^+}\frac{\partial V_\varphi^+}{\partial \varphi_+} + \frac{V_x^+}{r^+}\frac{dr^+}{dx_+} = 0 \qquad (2)$$

$$V_x^+\frac{\partial V_x^+}{\partial x_+} + V_y^+\frac{\partial V_x^+}{\partial y_+} + \frac{V_\varphi^+}{r^+}\frac{\partial V_x^+}{\partial \varphi_+} - \frac{V_\varphi^{+2}}{r_+}\frac{dr^+}{dx_+} = S_x T^+ + \frac{\partial^2 V_x^+}{\partial y_+^2} \qquad (3)$$

$$V_x^+\frac{\partial V_\varphi^+}{\partial x_+} + V_y^+\frac{\partial V_\varphi^+}{\partial y_+} + \frac{V_\varphi^+}{r^+}\frac{\partial V_\varphi^+}{\partial \varphi_+} + \frac{V_x^+ V_\varphi^+}{r^+}\frac{dr^+}{dx_+} = S_\varphi T^+ + \frac{\partial^2 V_\varphi^+}{\partial y_+^2} \qquad (4)$$

$$V_x^+\frac{\partial T^+}{\partial x_+} + V_y^+\frac{\partial T^+}{\partial y_+} + \frac{V_\varphi^+}{r^+}\frac{\partial T^+}{\partial \varphi_+} = \frac{1}{Pr}\frac{\partial^2 T^+}{\partial y_+^2} \qquad (5)$$

With $Pr = \frac{\mu Cp}{\lambda} = \frac{\nu}{a}$ and $Gr = \frac{g\beta(T_p - T_\infty)L^3}{\nu^2}$

Nusselt number and friction coefficients expressions

$$NuGr^{-\frac{1}{4}} = -\left(\frac{\partial T^+}{\partial y_+}\right)_{y_+=0}; Cf_u = Lc_f\left(\frac{\partial V_x^+}{\partial y_+}\right)_{y_+=0} \text{ and } Cf_\varphi = Lc_f\left(\frac{\partial V_\varphi^+}{\partial y_+}\right)_{y_+=0} \quad (6)$$

Lc_f is a coefficient which results from the adimensionnalisation.

Conditions to the limits

At the wall ($y^+ = 0$): $T^+ = 1, V_x^+ = 0, V_y^+ = 0$ et $V_\varphi^+ = 0$ (7)

Away from the wall ($y^+ \to \infty$): $T^+ \to 0, V_x^+ \to 0, V_y^+ \to 0$ and $V_\varphi^+ \to 0$ (8)

b. Case of pure rotary convection

The appropriate reduced variables are [21, 22]:

$$x^+ = \frac{x}{L}, y^+ = \frac{y}{L}\sqrt{Re_{e\omega}}, r^+ = \frac{r}{L}, V_x^+ = \frac{V_x}{L\omega}Re_\omega^{\frac{1}{4}}, V_y^+ = \frac{V_y}{L\omega}Re_\omega^{\frac{3}{4}}, V_\varphi^+ = \frac{V_\varphi}{L\omega}Re_\omega^{\frac{1}{4}}$$

$$\text{and } T^+ = \frac{T - T_\infty}{\left(\frac{L^2\omega^2}{2Cp}\right)} \quad (9)$$

Conditions to the limits

At the wall ($y^+ = 0$): $T^+ = 1, V_x^+ = 0, V_y^+ = 0$ and $V_\varphi^+ = 0$ (10)

Away from the wall ($y^+ \to \infty$): $T^+ \to 0, V_x^+ \to 0$ and $V_\varphi^+ \to 0$ (11)

c. Case of pure forced convection

The appropriate reduced variables are [10]:

$$x_+ = \frac{x}{L}, y_+ = \frac{y}{L}\sqrt{Re_\infty}, \varphi_+ = \varphi, r_+ = \frac{r}{L}, V_x^+ = \frac{V_x}{U_\infty}, V_y^+ = \frac{V_y}{U_\infty}\sqrt{Re_\infty},$$

$$V_\varphi^+ = \frac{V_\varphi}{U_\infty}, Ue^+ = \frac{Ue}{U_\infty}, Ue_x^+ = \frac{Ue_x}{U_\infty}, Ue_\varphi^+ = \frac{Ue_\varphi}{U_\infty} \text{ and } T^+ = \frac{T - T_\infty}{T_p - T_\infty} \quad (12)$$

Conditions to the limits

At the wall ($y^+ = 0$): $T^+ = 1, V_x^+ = 0, V_y^+ = 0$ and $V_\varphi^+ = 0$ (13)

Away from the wall ($y^+ \to \infty$): $T^+ \to 0, V_x^+ \to Ue_x$ and $V_\varphi^+ \to Ue_\varphi$ (14)

d. First case of mixed convection: natural and forced

Dimensionless reference quantities [23]:

$$\Delta T = T_P - T_\infty, x^+ = \frac{x}{L}, y^+ = C_1\frac{y}{L}, \varphi^+ = \varphi, r^+ = \frac{r}{L}, T^+ = C_5\frac{T}{\Delta T}, \quad (15)$$

$$V_x^+ = C_2\frac{V_x}{U_\infty}, V_y^+ = C_3\frac{V_y}{U_\infty}, V_\varphi^+ = C_2\frac{V_\varphi}{U_\infty}, Ue^+ = C_4\frac{Ue}{U_\infty}, Ue_x^+ = C_4\frac{Ue_x}{U_\infty} \text{ and } Ue_\varphi^+ = C_4\frac{Ue_\varphi}{U_\infty}$$

C_1, C_2, C_3, C_4 and C_5 are the barycentric coefficients of the mixed convection to manage the predominance.

Conditions to the limits

At the wall ($y^+ = 0$): $T^+ = 1, V_x^+ = 0, V_y^+ = 0$ and $V_\varphi^+ = 0$ (16)

Away from the wall ($y^+ \to \infty$): $T^+ \to 0, V_x^+ \to \left(\frac{C_2}{C_4}\right)Ue_x^+$ and $V_\varphi^+ \to \left(\frac{C_2}{C_4}\right)Ue_\varphi^+$ (17)

e. Second case of mixed convection: natural and rotary

Dimensionless reference quantities [24, 25]:

$$\Delta T = T_P - T_\infty, x^+ = \frac{x}{L}, y^+ = C_1\frac{y}{L}, \varphi^+ = \varphi, r^+ = \frac{r}{L}, V_x^+ = C_2\frac{V_x}{L\omega}, V_y^+ = C_3\frac{V_y}{L\omega}, V_\varphi^+ = C_2\frac{V_\varphi}{L\omega} \text{ and}$$

$$T^+ = \frac{T - T_\infty}{\Delta T} \quad (18)$$

Conditions to the limits

At the wall ($y^+ = 0$): $T^+ = 1, V_x^+ = 0, V_y^+ = 0$ and $V_\varphi^+ = C_2 r^+$ (19)

Away from the wall ($y^+ \to \infty$): $T^+ \to 0, V_x^+ \to 0$ and $V_\varphi^+ \to 0$ (20)

f. Third case of mixed convection: forced and rotary

Dimensionless reference quantities [26]:

$$x_+ = \frac{x}{L}, y_+ = \frac{y}{L}\sqrt{Re_\infty}C_1, \varphi_+ = \varphi, r_+ = \frac{r}{L}, V_x^+ = \frac{V_x}{U_\infty}C_2, V_y^+ = \frac{V_y}{U_\infty}\sqrt{Re_\infty}C_3, V_\varphi^+ = \frac{V_\varphi}{U_\infty}C_2$$

$$Ue^{+} = \frac{Ue}{U\infty} C_4,\ Ue_x{}^{+} = \frac{Ue_x}{U\infty},\ Ue_\varphi{}^{+} = \frac{Ue_\varphi}{U\infty} \text{ and } T^{+} = \frac{T - T\infty}{\Delta T} C_5 \quad (21)$$

Conditions to the limits

At the wall ($y^+ = 0$): $T^+ = 1$, $V_x{}^+ = 0$, $V_y{}^+ = 0$ and $V_\varphi{}^+ = C_2 r^+$ (22)

Away from the wall ($y^+ \to \infty$): $T^+ \to 0$, $V_x^+ \to \left(\frac{C_2}{C_4}\right) Ue_x^+$ and $V_\varphi^+ \to \left(\frac{C_2}{C_4}\right) Ue_\varphi^+$ (23)

V. METHODOLOGY AND MODELING

The study field is broken down into N x M x L curvilinear parallelepipeds attached to the body and defined by the dimensionless steps Δx_+, Δy_+ and $\Delta\varphi_+$. In this case, L and N are fixed in advance (Np, Nm), because they are directly related to the body geometric discretization. However, for a given stack indexed by p, the thickness of the boundary layer is not known in advance and the index (JMAX)p characterizes the thickness and changes a priori from one stack to another. Then, M is thus defined by the relation:

$$M = \sum_{p=1}^{LxN} (JMAX)p \quad (24)$$

Calculations are performed at nodes (i+1, j, k), with $1 \le i \le IMAX$, $1 \le j \le JMAX$ and $1 \le k \le KMAX$. For dimensionless quantities $V_x^+, V_y^+, V_\varphi^+$ and T^+, authors approximate the partial derivatives as follows, X designating one of them and the unknowns being the quantities indexed by i+1.
authors denote by U, V, W and T the meridian, normal, azimuthal components and the dimensionless temperature. After arrangement, the discretized equations can respectively be put in the following form:

$$AX_{j+1} + BX_j + CX_{j-1} = D_j, \text{ for } 2 \le j \le J\max - 1 \quad (25)$$

The algebraic systems (25) associated with the discretized boundary conditions are solved by the Thomas algorithm. As for the dimensionless normal component, it is obtained from the discretization of the continuity equation:

$$V_{i+1,j}^k = \frac{1}{4}\left[3V_{i+1,j+1}^k + V_{i+1,j-1}^k + 2\Delta y_+ \left(\frac{U_{i+1,j}^k - U_{i,j}^k}{\Delta x_+} + \frac{3W_{i+1,j}^{k+1} - 4W_{i+1,j}^k + W_{i+1,j}^{k-1}}{2\Delta\varphi_+ r_{i+1}^+} + \frac{U_{i+1,j}^k}{\Delta x_+}\left(1 - \frac{r_i^+}{r_{i+1}^+}\right)\right)\right] \quad (26)$$

In the calculations, authors took a precision $\varepsilon = 10^{-6}$ and the convergence criterion within the boundary layer is ensured when:

$$\left|\frac{|(X)^{p+1}| - |(X)^p|}{Sup(|(X)^{p+1}|, |(X)^p|)}\right| \le \varepsilon \quad (27)$$

$(X)^p$ and $(X)^{p+1}$ are respectively the values of the quantity X at iterations p and p+1.

VI. RESULTS AND DISCUSSION

Authors validated our calculation code with [27] for the cone case and with [28, 29] for the ellipsoid case in order to prove the accuracy of our results and the relative deviation not exceeding 1%.

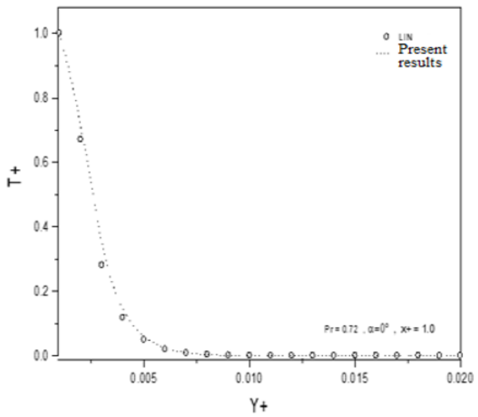

α_e	Present results	M. K. Jaman *et al.* (2010)	J. H Merkin (1977)
0.0	0.8412	0.8426	0.8359
0.2	0.7714	0.7706	0.7682
0.4	0.6622	0.6619	0.6617
0.6	0.5790	0.5781	0.5788
0.8	0.5184	0.5175	0.5187
1.0	0.4736	0.4729	0.4745
1.2	0.4397	0.4392	0.4409
1.4	0.4146	0.4132	0.4149
1.6	0.3936	0.3929	0.3943
1.8	0.3772	0.3768	0.3779
2.0	0.3644	0.3641	0.3646
2.2	0.3539	0.3538	0.3538
2.4	0.3450	0.3451	0.3447
2.6	0.3368	0.3370	0.3363
2.8	0.3264	0.3270	0.3266
3.0	0.3072	0.3062	0.3084
π	0.2782	0.2780	0.2785

(a) (b)

(a): Steady state temperature against y+, x+=1.0 and α=0°
(b): Numerical values of the heat exchange coefficient, $\alpha_e \epsilon [0, \pi]$, Pr=1.0 and b/a=0.25
Figure 2. Comparisons of the steady state temperature and exchange coefficient.

Generally, the growth of the rotation parameter and the opening attenuates the thickness of the thermal boundary layer (Figures 3). The reduction in thickness of the dynamic and thermal layers contributes to the stability of the entire sensor system and also marks the need to use the profile studied, taking into account the following correlations [30]:

$\theta_{0\ limit} = \pi/2 - (\alpha-1)$, for the tangential component and $\alpha \leq 45°$; (28)
$\theta_{0\ limit} \geq \alpha+1$, for the normal component. (29)

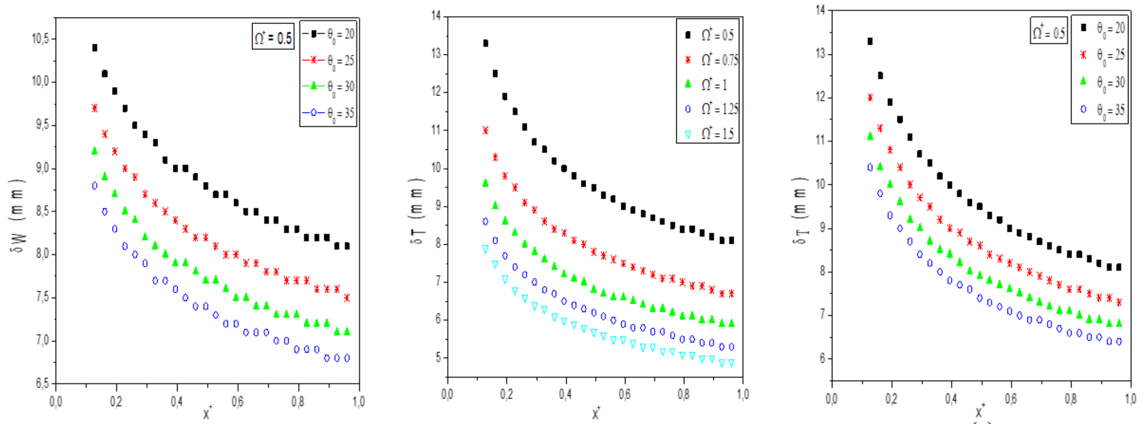

(a) (b) (c)

(a): Dynamic boundary layer, Ω+ = 0.5 and several values of θ_0
(b): Thermal boundary layer, for several values of Ω+.
(c): Thermal boundary layer, for several values of θ_0 and Ω+ = 0.5
Figure 3. Boundary layer thickness as a function of x+.

There is a zone on the wall of the profile, inert or in motion where the shape and position parameters have no influence on the normal component of the velocity, this zone is slippery according to the meridian coordinate x+ and the growth of this attenuates the amplitude of the aforementioned component. This point is collectively called a privileged point defined in the vicinity of equation φ=90° (figure 4.a). This area could open another field of research contributing to the improvement of the performance of aerodynamic profiles, even hydrodynamics. The range of use of flattening and opening the body is limited to 90° for a non-tilted body, and beyond this value, suction begins, and at 180°, the extent of this latter will cause instability harming the structure. The flat angle indicates the absence of the profile and the suction power is of magnitude and ready to give rise to turbulence, which represents a danger to the whole system (figures 4.b and 4.c).

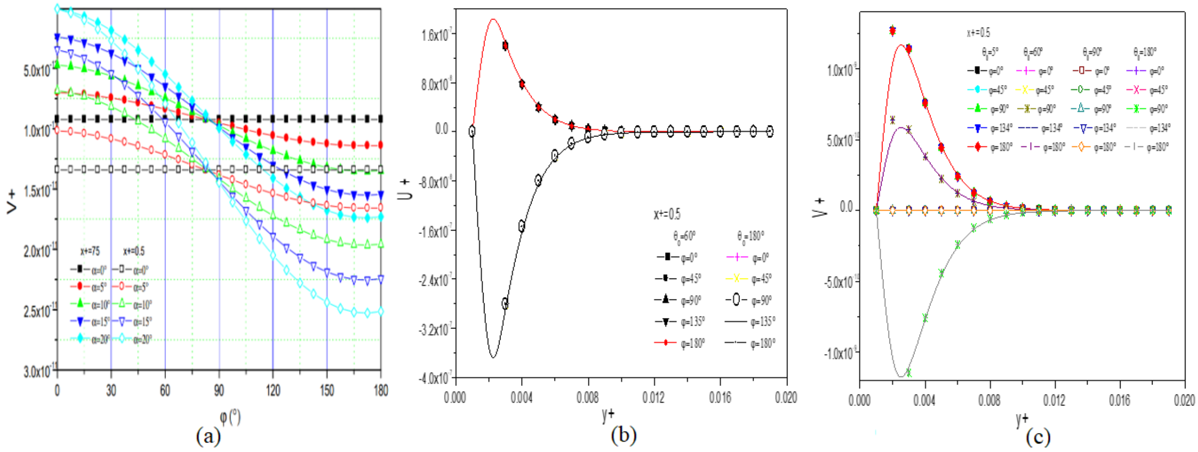

(a): V+ as a function of φ, for several values of α and x+

(b): U+ as a function of y+, for several values of φ, θ_0=60° and 180°, x+=0.5

(c): V+ as a function of y+, for several values of φ, θ_0=5°, 60°, 90° and 180°, x+=0.5

Figure 4. Evolution of the meridian and normal component of the velocity.

The flow would only be stable from 5° to 90°, which demystifies the choice of pattern manufacturers, of a current angle being around 60°, given the inclination $\alpha \leq 45°$ in our case, so that the profile could contribute to the straightening of the fluid net passing by this one as rectifier, stabilizer and current channeler towards the sensor to the good and ideal optimization of the wind motor operation.

VII. CONCLUSION AND PERSPECTIVE

Numerous examinations have been carried out through thousands of results derived from various cases, from several authors in the field of transfer by external convection, to answer a research question that offers an alliance between fundamental and applied research. The existence of the conical or elliptical shape at the entrance of wind turbines is not by chance or for aesthetic reasons, but it plays a crucial role in the stability of the whole aeromechanical wheel despite the absence of writings on it. In the majority of the cases approached, a parietal privileged point is seen on the normal component and this represents another door of investigation to the discovery of another scientific knowledge by posing another research question on the independence of a quantity dynamic in relation to shape and position parameters, how important and useful as a perspective.

Finally, this paper will contribute to the theoretical and conceptual aspect of the conical and elliptical shape of the wind turbines nose at both industrial and domestic scales. The proposed correlations limiting the intensity of the tangential and normal dynamic quantities are conceptually recommended to limit the importance of suction and adhesion caused by the particle's confinement. The coupling two by two of the identified convection typology will certainly contribute to the new techno-scientific knowledge responding to the improvement of the wind turbine aerodynamic performance.

REFERENCES

[1]. Assembly of a JUVENT wind turbine on site (Mont-Crosin, Switzerland, near Bern): https://www.youtube.com/watch?v=iceJfv58bAQ, and EDF video that summarizes the operation of a wind turbine: https://www.youtube.com/watch?v=v6ZNDQ80ELE. Accessed June 25, 2022.

[2]. H.J. Merk and J. A. Prins, (1953). Thermal convection in laminar boundary layer. Int. Appl. Sci. Res., 4, pp.11-24.

[3]. M. A. Hossain and S. C. Paul, (2001). Free convection from a vertical permeable circular cone with nonuniform surface temperature. Acta Mechanica, 151, pp. 103-114.

[4]. M. Alamgir, (1989). Overall heat transfer from vertical cones in laminar free convection: an approximate method. ASME Journal of Heat Transfer, 101, pp. 174-176.

[5]. B. Pullepu, K. Ekambavanan and A. J. Chamkha, (2007). Unsteady laminar natural convection flow past an isothermal vertical cone. Int. J. Heat and Technology, 25(2), pp.17-28.

[6]. Pop and T. Yen, (1999). Natural convection over a vertical wavy frustum of a cone. Int. J. Non-linear Mechanics, 34, pp. 925-934.

[7]. Y. C. Ching, (2015). Free convection heat transfert from a non-isothermal. Permeable cone suction and temperature dependent viscosity. Journal of applied Science andEngineering, 18(1), pp. 17-24.

[8]. M. Siabdallah, B. Zeghmati and M. Daguenet. Etude de la convection naturelle thermique et massique dans la couche limite autour d'un tronc de cône à paroi sinusoïdale. 12è Journée Internationale de Thermique, Maroc, 2005.

[9]. H. Abdurrachim. Etude théorique et expérimentale de la convection naturelle laminaire sur des surfaces ondulées. Doctoral thesis, Perpignan University, France, 1980.

[10]. F. A. Rakotomanga and E. Alidina. Transferts thermiques convectifs tridimensionnels autour d'un cône de révolution. Conference SFT, réf 6212, Gérardmer, France, 2013.

[11]. S. Nadeem, S. Saleem, (2014). Mixed convection flow of Eyring – Powell fluid along a rotating cone", Result in Physics, 4, pp. 54-62.
[12]. Y. Mochimaru. Numerical Simulation of Natural Convection in a Cavity of an Ellipsoid of Revolution, using a Spectral Finite Difference Method. Fourteenth International Conference on Numerical Methods in Fluid Dynamics, India, 453, pp. 485-489, 2005.
[13]. M. Medvinsky, E. Turkel and U. Hetmaniuk, (2008). Local absorbing boundary conditions for elliptical shaped boundaries. JCP, 227(18), pp. 8254-8267.
[14]. N. Souad, C. Mbow, J. H. Lee, W. H. Park and M. Daguenet, (1990). Etude numérique du modèle de Boussinesq de convection naturelle transitoire dans un ellipsoide de révolution de grand axe vertical rempli d'air. JHT, 36(3), pp.224-233.
[15]. N. Souad. Etude numérique de la convection naturelle dans un ellipsoïde de révolution de grand axe vertical et dans un cylindre horizontal de section elliptique. Doctoral thesis, Perpignan University, France, 1996.
[16]. C. Raminosoa, R. Ratobison, A. Ali cherif, A. Daif and M. Daguenet, (1995). Convection mixte autour d'une sphère, Revue Générale de Thermique.
[17]. E. Alidina. Contribution à l'étude d'une convection mixte tridimensionnelle autour d'une ellipsoïde de révolution dans un écoulement ascendant de fluide newtonien, Doctoral thesis, Antananarivo University, Madagascar, 1997.
[18]. G. Le Palec, (1986). Etude de la convection mixte tridimensionnelle autour d'une sphère en rotation dans un écoulement ascendant de fluide newtonien. Doctoral thesis, Perpignan University, France, 1986.
[19]. D. Ouldhadda, Etude de la convection mixte autour d'un corps à symétrie de révolution d'axe vertical en rotation en présence d'un écoulement forcé axial et d'une convention naturelle, Doctoral thesis, Perpignan University, France, 1991.
[20]. U. Canissius, F. A. Rakotomanga and E. Alidina (2015). Etude numérique de la convection naturelle tridimensionnelle autour d'un cône de révolution inclinée. Afrique SCIENCE, 11(1), pp. 1-11.
[21]. G. Bezandry, (2017.a). Influence de l'ouverture du sommet sur la convection rotatoire pure autour d'un cône de révolution. Afrique SCIENCE, 13(3), pp.251 - 261.
[22]. G. Bezandry,R. Randrianarivelo, C. Leticia, E. K.Mourtallah-x, U.Canissius and E.Alidina, (2017.b). Influence de l'écoulement forcée sur la convection rotatoire autour d'un cône de révolution. Afrique SCIENCE, 13(4), pp. 357 - 368.
[23]. E. Mourtallah-x, F. A. Rakotomanga, U. Canissius and E. Alidina, (2019). Numerical study of the three-dimensional mixed convection around an inclined cone of revolution. American Journal of Engineering Research, 8(5), pp. 150-160.
[24]. R. Randrianarivelo, G. Bezandry, U. Canissius and E. Alidina, (2017). Convection mixte tridimensionnelle, naturelle et rotatoire autour d'un cône. Afrique SCIENCE, 13(5), pp. 150-160.
[25]. R. Randrianarivelo, G. Bezandry, U. Canissius and E. Alidina, (2018). Étude d'une convection mixte tridimensionnelle naturelle et rotatoire autour d'un cône incliné. Afrique SCIENCE, 14(1), pp. 281-291.
[26]. C. Leticia, U. Canissius and E. Alidina, (2020). Forced and Rotary Convection around a Cone of Revolution. American Journal of Engineering Research, 9(11), pp. 48-53.
[27]. F. N. Lin, (1976). Laminar convection from a vertical cone with uniform surface heat flux. Letters in Heat and Mass Transfer, 3, pp. 49–58.
[28]. M. K. Jaman and M. A. Hossain, (2010). Effect of Fluctuating Surface Temperature on Natural Convection Flow Over Cylinders of Elliptic Cross Section. OTPJ, 2, pp. 35-47.
[29]. J.H. Merkin, (1977). Free convection boundary layers on cylinders of elliptic cross section, ASME JHT, 99, pp. 453–457.
[30]. U. Canissius. Convection naturelle tridimensionnelle autour d'un cône de révolution incliné. Doctoral thesis, Antsiranana University, Madagascar, p. 202, 2016.